Sensors and Materials, Vol. 17, No. 3 (2005) 155–165
MYU Tokyo

S & M 0594

Fabrication of 100-nm-Scale Nickel Stamper Based on Chrome/Quartz Mask without Anti-Reflection Layer

Young Ho Seo*, Doo-Sun Choi, Yeong-Eun Yoo, Joon-Hyoung Lee, Tae-Jin Je and Kyung-Hyun Whang

Intelligence and Precision Machine Department, Korea Institute of Machinery & Materials, 171 Jang-dong, Yuseong-gu, Daejeon 305-343, Republic of Korea

(Received April 10, 2004; accepted December 20, 2004)

Key words: nickel stamper, e-beam lithography, injection molding, 100-nm-scale stamper.

We present a fabrication method for a high-aspect-ratio 100-nm-scale nickel stamper using e-beam writing on a chrome/quartz mask for the injection molding of optical grating patterns. We suggest a new fabrication process for a 100-nm-scale nickel stamper which uses a chrome layer on a blank mask as a seed layer for the nickel electroplating process. A conventional blank mask consists of layers in the order of Photoresist (PR), CrON and Cr on a quartz substrate (PR/CrON/Cr/Qz). We have prepared a blank mask without an antireflection layer of CrON, which is a nonconductive material, in order to use the chrome layer as a seed layer for the electroplating process. In PR mold fabrication, we have determined an optimum e-beam dosage of 10 $\mu C/cm^2$ for the PR/CrON/Cr/Qz mask, and one of 8.5 $\mu C/cm^2$ for the PR/Cr/Qz mask. The fabricated PR mold on the PR/CrON/Cr/Qz mask showed a minimum line width of 84 nm and the PR mold on the PR/Cr/Qz mask showed one of 96 nm with a height of 300±10 nm. We have deposited additional seed layer materials of Ni as thick as 100 nm due to the high electric resistance of the Cr layer of 100 Ω. After the nickel electroplating process, the total thickness of the fabricated nickel stamper was approximately 330±20 μm. The minimum width and height of the fabricated nickel line were measured as 116±6 nm and 240±20 nm, respectively. Consequently, we have fabricated a 2.5-AR (Aspect Ratio) nickel stamper with a minimum width of 116±6 nm. The fabricated 100-nm-scale nickel stamper showed a maximum error of 20 nm compared with the PR mold.

*Corresponding author, e-mail address: yhseo@kimm.re.kr

1. Introduction

Recently, many researchers have been interested in large scale and nanostructure fabrication technologies of back light units (BLUs) and optical gratings because of the increase in the demand for flat display panels. In this paper, we consider injection molding technology, which has several advantages such as size extension and low-cost manufacturing. For the injection molding process, a stamper made of electroplated nickel is required. Figure 1 shows the conventional fabrication procedure for a nickel stamper. After the photoresist coating process is performed on the quartz substrate, the photoresist is patterned by laser direct writing or electron beam writing, and the seed layer for the electroplating process is deposited. Finally, a nickel stamper is fabricated by the electroplating process using the photoresist mold and deposited seed layer.(1–4) In this nickel electroplating process, the seed layer deposition step is indispensable. A seed layer thickness of 50 nm ~ 300 nm may cause dimension error after the fabrication of the 100-nm-scale nickel stamper. On other hand, microfluidic and optical devices such as the lab-on-a-chip, optical switches and lenses have been fabricated by the micromolding technique. The minimum feature size of these devices is in the range of 10 μm ~ 100 μm. In these cases, stampers for the micromolding process were fabricated by the ultraviolet (UV) lithography process using a polymer such as SU-8.(5,6) Actually, the polymer(SU-8) stamper does not have sufficient strength and melting temperature for polycarbonate and polymethylmethacrylate (PMMA) to be used as replica materials. When we want to use a polymer stamper, we must use soft replica materials such as polydimethylsiloxane (PDMS) and rubber.

In this paper, we suggest a new fabrication process for a 100-nm-scale nickel stamper. By using a chrome layer on a blank mask as a seed layer for the electroplating process, we would like to simplify the nickel stamper fabrication process and improve the accuracy of the fabricated nickel stamper. Generally, a blank mask used in the lithography process consists of a chrome layer and a photoresist layer on a quartz substrate. The chrome layer is composed of a UV antireflection layer of CrON and a UV shade layer of Cr(94%Cr-

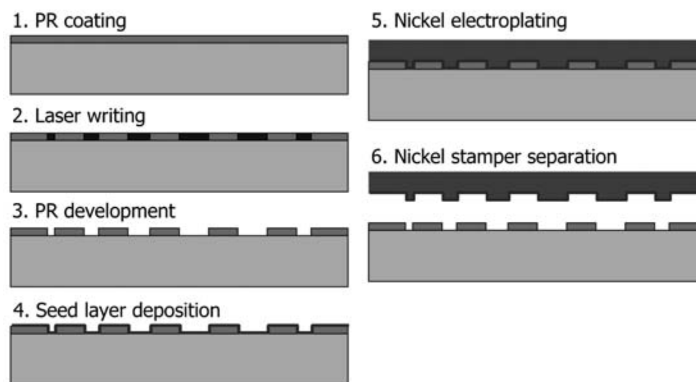

Fig. 1. Fabrication process of conventional nickel stamper.

6%C).(7,8) The UV antireflection layer of CrON absorbs UV light in the UV lithography process in order to prevent interference between the incident and reflected light. As shown in Fig. 2(a), a conventional blank mask consists of layers in the order of PR, CrON and Cr on a quartz substrate (PR/CrON/Cr/Qz blank mask). However, the antireflection layer of CrON is electrically a nonconductive material. Therefore, we have prepared a blank mask without the antireflection layer of CrON (PR/Cr/Qz blank mask) in order to use the chrome layer as a seed layer for the electroplating process, as shown in Fig. 2(b).

The mask fabrication process using electron beam writing is generally optimized on the basis of the PR/CrON/Cr/Qz blank mask. Therefore, we have to determine the optimum electron beam dosage for the PR/Cr/Qz blank mask. Figures 1 and 3 show the conventional nickel stamper fabrication process using the laser writing process on the PR on the glass substrate and the present nickel stamper fabrication process using electron beam writing based on the PR/Cr/Qz blank mask, respectively. As shown in Fig. 3, we can simplify the nickel electroplating process and improve the accuracy of the nickel stamper because we can carry out the electroplating process without any seed layer deposition process.

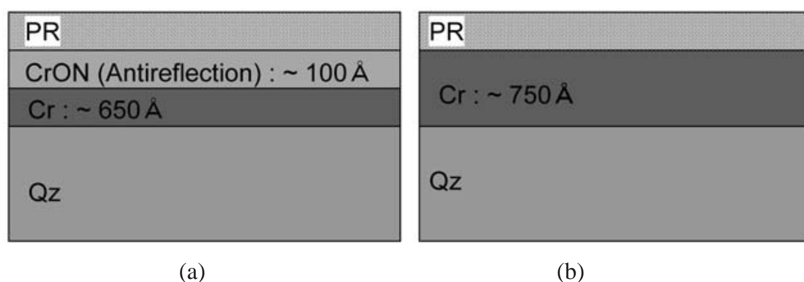

(a) (b)

Fig. 2. Comparison of configuration of blank masks: (a) conventional blank mask with antireflection layer (PR/CrON/Cr/Qz blank mask); (b) blank mask without antireflection layer (PR/Cr/Qz blank mask).

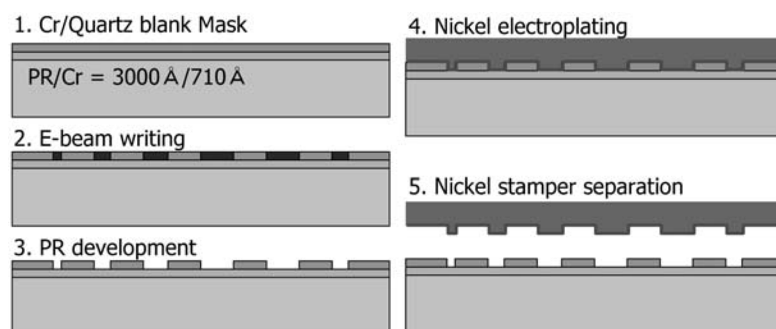

Fig. 3. Fabrication process of present nickel stamper based on PR/Cr/Quartz blank mask.

2. Test Specimen Design

We have designed four different types of test specimens including 0.5-mm-pitch(line+space), 1.0-µm-pitch, 2.0-µm-pitch and 4.0-µm-pitch specimens. Figures 4 and 5 show the overall view of the 6-inch mask layer and the enlarged view of type 1 of the 0.50 mm pitch specimen. The size of each type of specimen is 10 mm × 10 mm. In the case of type 1, we have changed the line width from 100 nm to 400 nm in 9 steps. Similarly, the other types have 9 different lines and spaces as shown in Table 1. Lines and spaces in the PR mold will result in spaces and lines, respectively, in the nickel stamper, after the nickel electroplating process.

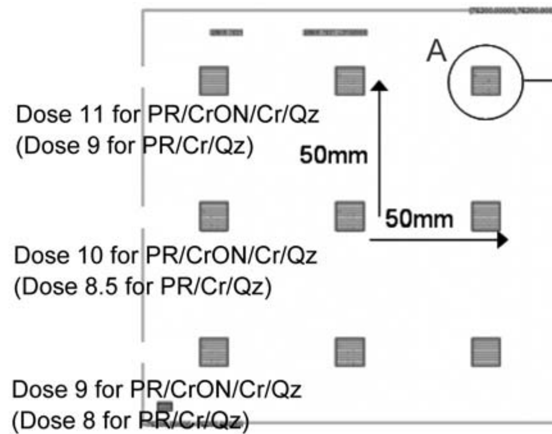

Fig. 4. Overall view of blank mask layout for optimizing e-beam dosage.

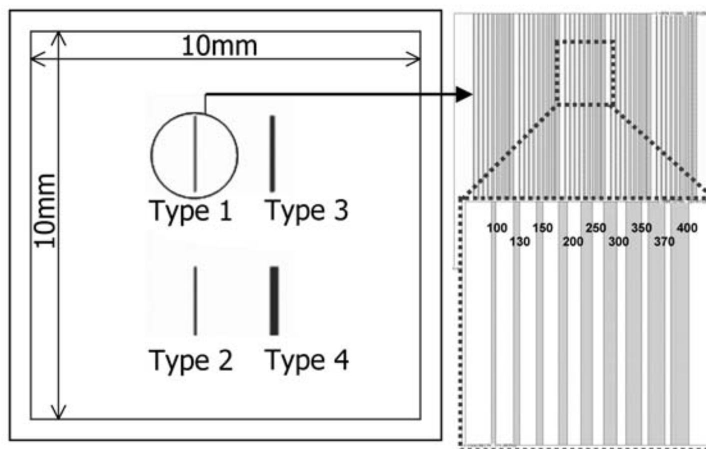

Fig. 5. Enlarged view of test specimen of A-region shown in Fig. 4 and type 1.

Table 1
Dimensions of nano-grating structure shown in Fig. 5.

Type 1 (pitch:0.5 mm)		Type 2 (pitch:1.0 mm)		Type 3 (pitch:2.0mm)		Type 4 (pitch:4.0 mm)	
Line	Space	Line	Space	Line	Space	Line	Space
0.10	0.40	0.1	0.9	0.1	1.9	0.1	3.9
0.13	0.37	0.2	0.8	0.3	1.7	0.5	3.5
0.15	0.35	0.3	0.7	0.5	1.5	1.0	3.0
0.20	0.30	0.4	0.6	0.7	1.3	1.5	2.5
0.25	0.25	0.5	0.5	0.9	1.1	2.0	2.0
0.30	0.20	0.6	0.4	1.1	0.9	2.5	1.5
0.35	0.15	0.7	0.3	1.3	0.7	3.0	1.0
0.37	0.13	0.8	0.2	1.5	0.5	3.5	0.5
0.40	0.10	0.9	0.1	1.7	0.3	3.9	0.1

In the fabrication of the PR mold, we used two different blank masks, namely the PR/CrON/Cr/Qz blank mask and the PR/Cr/Qz blank mask, to verify the effect of the CrON layer in electron beam lithography. In order to find the optimum dosage of the electron beam for the two masks, we divided each 6-inch mask into 3 different regions which were each exposed to the same dosage of the electron beam, as shown in Fig. 4. We have inserted notes detailing the three different dosages of the electron beam for the PR/CrON/Cr/Qz blank mask as well as the dosages of the electron beam for the PR/Cr/Qz blank mask in parentheses. The thicknesses of the PR, CrON and Cr layers in the PR/CrON/Cr/Qz blank mask are approximately 300 nm, 10 nm and 65 nm, respectively. In case of the PR/Cr/Qz blank mask, the thickness of the PR layer is 300 nm, and the thickness of the Cr layer is approximately 75 nm.

3. Experimental Results

3.1 *PR mold*

First, we fabricated a PR mold for the nickel electroplating process. For the conventional PR/CrON/Cr/Qz blank mask, we initially decided that the dosages of the electron beam should be 11 $\mu C/cm^2$, 10 $\mu C/cm^2$, and 9 $\mu C/cm^2$ on the basis of the existing data from electron beam lithography. However, we finally decided that the dosages of the electron beam should be 9 $\mu C/cm^2$, 8.5 $\mu C/cm^2$, and 8 $\mu C/cm^2$ on the basis of several trial-and-error tests to determine the optimum dosages of the electron beam for the PR/Cr/Qz blank mask.

Figure 6 shows SEM images of the fabricated PR molds based on the PR/CrON/Cr/Qz blank mask and the PR/Cr/Qz blank mask. Figures 7 and 8 enable a comparison of the dimensions of the fabricated PR molds for the PR/CrON/Cr/Qz blank mask and PR/Cr/Qz blank mask, respectively.

For the PR/CrON/Cr/Qz blank mask, PR patterns were underdeveloped at the electro beam dosage of 9 $\mu C/cm^2$, overdeveloped at 11 $\mu C/cm^2$, and optimally developed at 10 $\mu C/cm^2$. Under the optimum condition of 10 $\mu C/cm^2$, the minimum line width of the fabricated

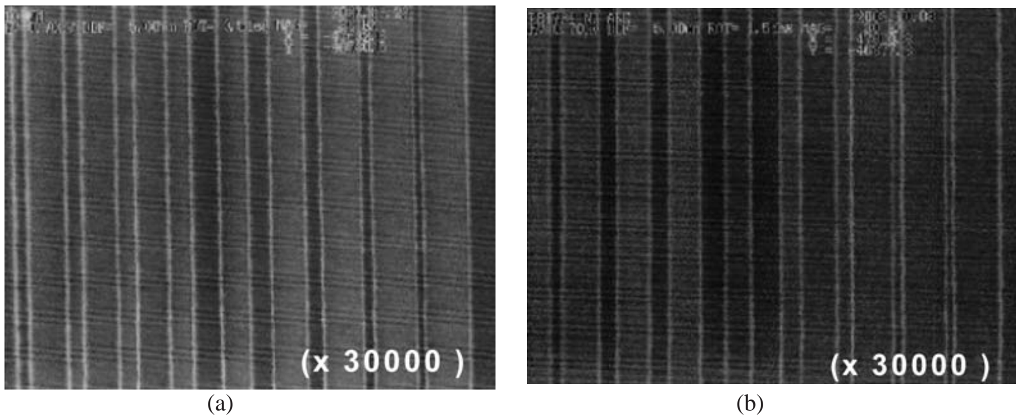

(a) (b)

Fig. 6. SEM images of fabricated PR mold using blank mask and e-beam lithography : (a) PR mold of PR/CrON/Cr/Qz blank mask at 10 μC/cm^2; (b) PR mold of PR/Cr/Qz blank mask at 8.5 μC/cm^2.

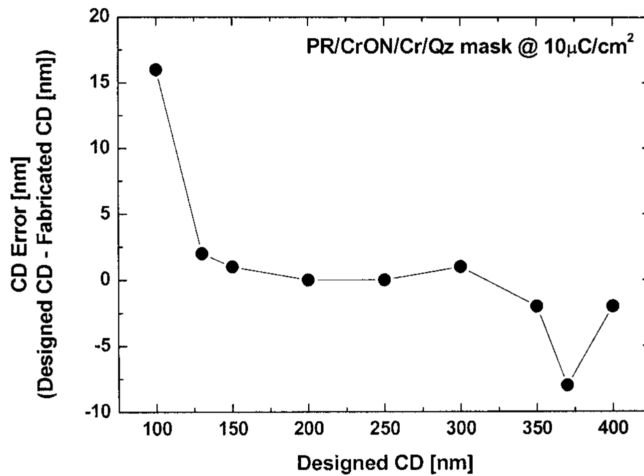

Fig. 7. Comparison of designed PR line width with measured PR line width of type 1 specimen in PR/CrON/Cr/Qz blank mask at optimal e-beam dose of 10 μC/cm^2: maximum error in type 1 is 16 nm.

PR mold based on the PR/CrON/Cr Qz blank mask was 84 nm, and the maximum error of type 1 was 16 nm for the 100 nm line width, as shown in Fig. 7. On the other hand, the PR patterns on the PR/Cr/Qz blank mask were underdeveloped at an electron beam dosage of 8 μC/cm^2, overdeveloped at 9 μC/cm^2, and optimally developed at 8.5 μC/cm^2. Under the optimum condition of 8.5 μC/cm^2, the minimum line width was 96 nm, and the maximum error of type 1 was 24 nm for the 370 nm line, as shown in Fig. 8. The fabricated PR mold shows a height of 300±10 nm, which is lower than the initial PR thickness of the blank mask. These discrepancies between the PR mold and the initial PR layer may result from the dry or etching processes in the electron beam lithography process.

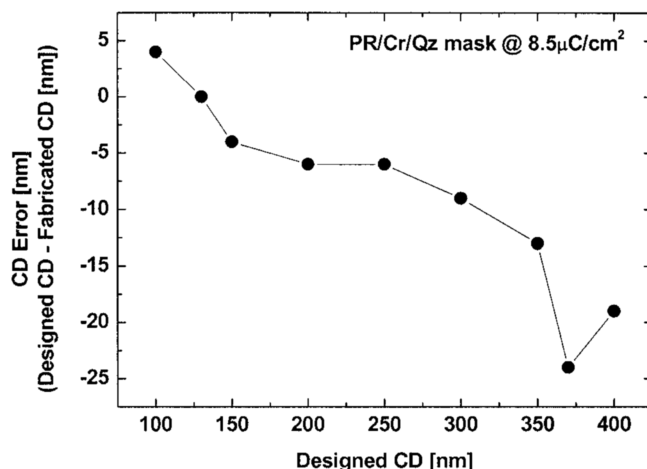

Fig. 8. Comparison of designed PR line width with measured PR line width of type 1 specimen in PR/Cr/Qz blank mask at optimal e-beam dose of 8.5 μC/cm^2: maximum error in type 1 is 24 nm.

From the experimental study of the fabrication of PR molds, we determined optimum patterning conditions for the cases of PR/CrON/Cr/Qz and PR/Cr/Qz blank masks. In the next step, we fabricated a nickel stamper using the fabricated PR mold on the PR/Cr/Qz mask without a seed layer deposition process.

3.2 *Nickel stamper*

The electric resistance of the Cr layer in the fabricated PR mold of the PR/Cr/Qz blank mask was measured as 100 Ω. In the electroplating process, unfortunately, the 75-nm-thick Cr layer underneath the PR of the PR/Cr/Qz blank mask was damaged due to high resistance, that is, a thickness of 75 nm was insufficient to protect the Cr layer from the electric field in the electroplating process. In this work, we deposited an additional seed layer of Ni with 100 nm thickness. Finally, we got a resistance of 10 Ω. Instead of a 75-nm-thick Cr layer, if we prepare a 200-nm-thick Cr layer PR/Cr/Qz blank mask, we can carry out the electroplating process without any additional seed layer deposition process.

The total thickness of the fabricated nickel stamper was approximately 330±20 μm. Figure 9 shows SEM images of the nickel stampers of types 1, 2, 3, and 4 fabricated using the PR/Cr/Qz blank mask. Figure 10 shows the SEM image of the nickel stamper fabricated using the PR/CrON/Cr/Qz blank mask. From SEM images of the PR mold and nickel stamper shown in Figs. 6, 9 and 10, we determined that the CrON layer did not make any difference in e-beam lithography and the nickel electroplating process. In the case of type 1, the minimum width of the fabricated nickel line was measured as 116±6 nm. Using a scanning probe microscope (SPM), we measured the height of the nickel line as 240±20 nm, as shown in Fig. 11. Because the fabricated nickel line has an aspect ratio (AR) of 2.5, the sharpness of the probe tip of the SPM was not sufficient to measure the shape of the nickel stamper. The height of the fabricated nickel line was less than that of the PR mold of 300±10 nm. In order to determine the reason why the nickel line was lower than the PR mold, we obtained an enlarged SEM image of the nickel stamper, as shown in Fig. 12. In

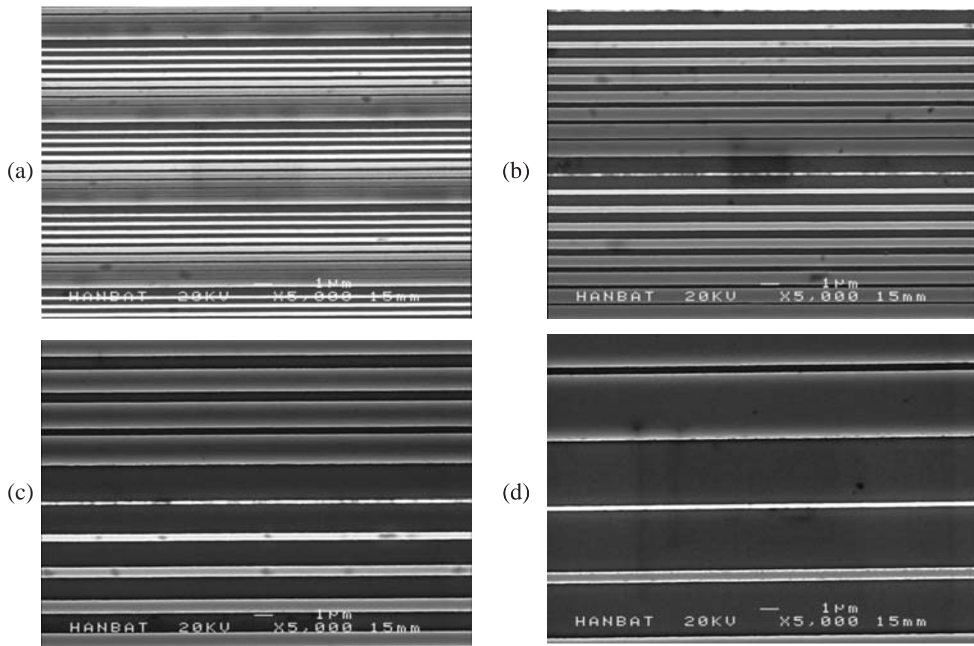

Fig. 9. SEM image of nickel stamper fabricated using PR/Cr/Qz blank mask: (a) Type 1: 0.5 μm-pitch, CD_{min}=0.1 μm, CD_{max}=0.4 μm; (b) Type 2: 1.0 μm-pitch, CD_{min}=0.1 μm, CD_{max}=0.9 μm; (c) Type 3: 2.0 μm-pitch, CD_{min}=0.1 μm, CD_{max}= 0.9 μm; (d) Type 4: 4.0 μm-pitch, CD_{min}=0.1 μm, CD_{max}=3.9 μm.

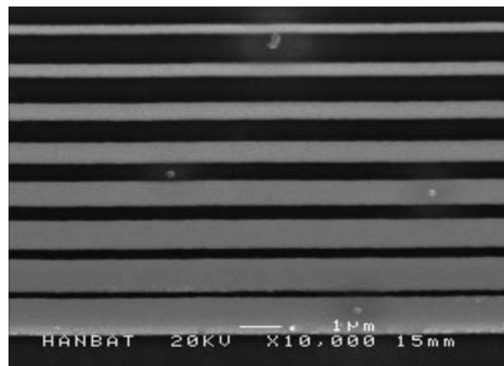

Fig. 10. SEM image of nickel stamper fabricated using PR/CrON/ Cr/Qz blank mask . (Type 4: 4.0 μm-pitch, CD_{min}=0.1 μm, CD_{max}=3.9 μm).

Fig. 12 we can see an additional nickel layer whose thickness is approximately 90±5 nm on both sides of the nickel line. This indicates that the additional nickel layer on top of the nickel line was attached to the Cr layer of the PR/Cr/Qz blank mask during the separation process of the nickel stamper and the PR/Cr/Qz blank mask. Consequently, the height of

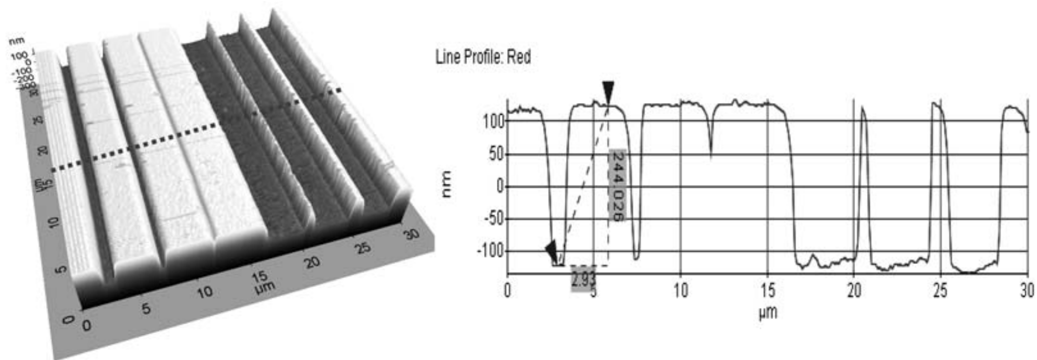

Fig. 11. AFM image of fabricated nickel stamper of type 4 in Fig. 9(d): the height of the nickel stamper is 240±20 nm.

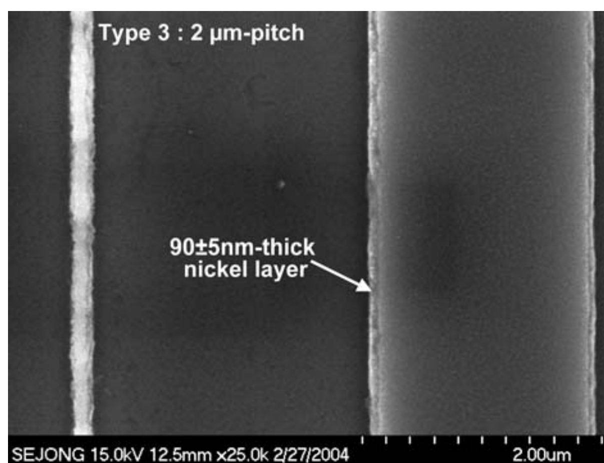

Fig. 12. SEM image of fabricated nickel stamper of type 3: additional deposited 90±5-nm-thick nickel layer can be observed.

the nickel line was lower than the designed height by as much as 60±20 nm. If we use a 200-nm-thick Cr layer for the PR/Cr/Qz blank mask, we can fabricate the nickel stamper without an additional seed layer deposition process. Therefore, the height of the nickel line can be accurately controlled by adjusting the thickness of the PR mold.

Figure 13 shows a comparison of the width of the fabricated nickel lines and the width of the PR mold for type 1. The minimum line width of the nickel stamper was 116±6 nm. From Fig. 13, we can determine that the fabricated nickel stamper shows a maximum error of 20 nm compared with the PR mold of type 1.

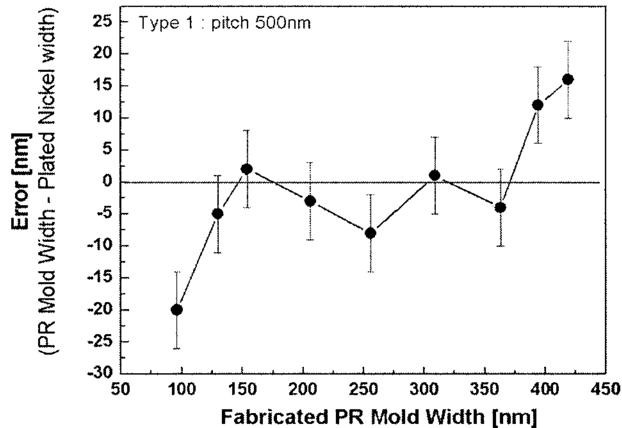

Fig. 13. Comparison of width of PR mold line at 8.5 μC/cm^2 with nickel stamper line of type 1 specimen: maximum error in type 1 is ±20 nm.

4. Conclusion

We presented a fabrication method for a high-aspect-ratio 100-nm-scale nickel stamper using e-beam writing on the chrome/quartz mask for the injection molding of optical grating patterns. In this study, we simplified the nickel stamper fabrication process and improved the accuracy of the fabricated nickel stamper by using a chrome layer on a blank mask as a seed layer for the electroplating process. In the PR mold fabrication process, we have determined an optimum e-beam dosage of 10 μC/cm^2 for the PR/CrON/Cr/Qz blank mask, and one of 8.5 mC/cm^2 for the PR/Cr/Qz blank mask. The fabricated PR mold on the PR/CrON/Cr/Qz blank mask showed the minimum line width of 84 nm and the PR mold on the PR/Cr/Qz blank mask showed one of 96 nm with the height of 300±10 nm. We fabricated a 330±20-μm-thick nickel stamper with a minimum width and height of the fabricated nickel line of 116±6 nm and 240±20 nm, respectively. Furthermore, we fabricated a 2.5-AR nickel stamper with a minimum width of 116±6 nm. The fabricated 100-nm-scale nickel stamper showed a maximum error of ±20 nm compared with the PR mold. Consequently, we have optimized the electron-beam dosage for the PR/Cr/Qz blank mask and fabricated a 100-nm-scale nickel stamper for optical grating patterns with a 2.5-AR.

Acknowledgments

This work has been supported by the 21st Century Frontier R&D Program of the Ministry of Science and Technology (MOST) under the project title of "Nanoscale Mechatronics and Manufacturing."

References

1 G. Timp: Nanotechnology, Springer. 1999.
2 T. G. Bifano, H. E. Fawcett and P. A. Bierden: Precision Engineering **20** (1997) 53.
3 Y. Kim, N. Lee, Y.-J. Kim and S. Kang: "Fabrication of metallic nano-stamper and replication of nano-patterned substrate for patterned media," NSTI-Nanotech 2004, pp.452-455, 2004.
4 S. Yoon, C. Srirojpinyo, J. Lee, C. Sung, J. L. Mead and M. F. Carol: "Investigation of tooling surfaces on injection molded Nanoscale features," NSTI-Nanotech 2004, pp.460-463, 2004.
5 I. Doh, K.-S. Seo, and Y.-H Cho: "A continuous cell separation chip using hydrodynamic dielectrophoresis process," IEEE MEMS 2004, pp.29-32, 2004.
6 K.-J. Jeong, G. L. Liu, N. Chronis and L. P. Lee: "Tunable microdoublet lens array," IEEE MEMS 2004, pp.37-40, 2004.
7 G. T. A. Kovacs: Micromachined Transducers, McGraw-Hill, 1998.
8 Y. Nakagawa, T. Komagata, Y. Kawase, and N. Gotoh: JEOL News 38 (2003).